G-Protein-Dependent Cell Surface Dynamics of the Human Serotonin$_{1A}$ Receptor Tagged to Yellow Fluorescent Protein†

Thomas J. Pucadyil,‡ Shanti Kalipatnapu,‡ Kaleeckal G. Harikumar,‡,§ Nandini Rangaraj,‡ Sadashiva S. Karnik,|| and Amitabha Chattopadhyay*,‡

Centre for Cellular and Molecular Biology, Uppal Road, Hyderabad 500 007, India, and Department of Molecular Cardiology, Lerner Research Institute, The Cleveland Clinic Foundation, Cleveland, Ohio 44195

Received September 5, 2004; Revised Manuscript Received October 13, 2004

ABSTRACT: Serotonergic signaling appears to play a key role in the generation and modulation of various cognitive, behavioral, and developmental processes. The serotonin$_{1A}$ receptor is an important member of the superfamily of seven transmembrane domain G-protein-coupled receptors and is the most extensively studied among the serotonin receptors. Several aspects of serotonin$_{1A}$ receptor biology such as cellular distribution and signal transduction characteristics are technically difficult to address in living cells on account of the inability to optically track these receptors with fluorescence-based techniques. We describe here the characterization of the serotonin$_{1A}$ receptor tagged to the enhanced yellow fluorescent protein (EYFP) stably expressed in Chinese hamster ovary (CHO) cells. These receptors were found to be essentially similar to the native receptor in pharmacological assays and can therefore be used to reliably explore aspects of receptor biology such as cellular distribution and dynamics on account of their intrinsic fluorescent properties. Analysis of the cell surface dynamics of these receptors by fluorescence recovery after photobleaching (FRAP) experiments has provided novel insight into the molecular mechanism of signal transduction of serotonin$_{1A}$ receptors in living cells. Interestingly, addition of pharmacologically well-characterized ligands or activators of G-proteins altered the diffusion characteristics of the receptor in a manner consistent with the G-protein activation model. These results demonstrate, for the first time, that membrane dynamics of this receptor is modulated in a G-protein-dependent manner.

The G-protein-coupled receptor (GPCR)[1] superfamily is one of the largest protein families in mammals (*1*). Signal transduction events mediated by this class of proteins are the primary means by which cells communicate with and respond to their external environment. This is achieved through the activation of GPCRs upon binding of ligands present in the extracellular environment which results in transduction of signals to the interior of the cell through concerted changes in their transmembrane domain structure (*2*). The major paradigm in this signal transduction process is that stimulation of GPCRs leads to the recruitment and activation of the heterotrimeric GTP-binding proteins (G-proteins) (*3*). The activation process stimulates the GDP−GTP exchange leading to the dissociation of the GTP-bound α-subunit and the $\beta\gamma$-dimer of the G-protein from the GPCR.

These initial events, which are fundamental to all types of GPCR signaling, occur at the plasma membrane via protein−protein interactions. An important consequence of this is that the dynamics of the activated receptor on the cell surface represents an important determinant in its encounter with G-proteins and has significant impact on the overall efficiency of the signal transduction process. This aspect forms the basis of the "mobile receptor" hypothesis in which the lateral mobility of the receptor on the cell surface is assumed to play an important role in cellular signaling (*4*). This model proposes that receptor−effector interactions at the plasma membrane are controlled by lateral mobility of the interacting components. Evidence for this comes from previous reports in which the ability of vasopressin V_2 receptors to activate adenylate cyclase through G-proteins was found to be directly dependent on the mobile fraction of these receptors on the cell surface (*5*), and the activation of G-proteins by light-activated rhodopsin was determined

† Supported by research grants from the Council of Scientific and Industrial Research, Government of India, to A.C., RO1 Grant HL57470 to S.S.K. from the National Institutes of Health, and CAEN grant from the International Society for Neurochemistry to S.K. T.J.P. and S.K. thank the Council of Scientific and Industrial Research for the award of Senior Research Fellowships. K.G.H. thanks the Council of Scientific and Industrial Research for the award of a Research Associateship. S.S.K. is an Established Investigator Award recipient from the American Heart Association.

* To whom correspondence should be addressed. Telephone: +91-40-2719-2578. Fax: +91-40-2716-0311. E-mail: amit@ccmb.res.in.

‡ Centre for Cellular and Molecular Biology.

§ Present address: Cancer Center and Department of Molecular Pharmacology and Experimental Therapeutics, Mayo Clinic, Scottsdale, AZ 85259.

|| The Cleveland Clinic Foundation.

[1] Abbreviations: 5-HT, 5-hydroxytryptamine; 5-HT$_{1A}$ receptor, 5-hydroxytryptamine 1A receptor; 5-HT$_{1A}$R-EYFP, 5-hydroxytryptamine 1A receptor tagged to EYFP; 8-OH-DPAT, 8-hydroxy-2-(di-*N*-propylamino)tetralin; BCA, bicinchoninic acid; EYFP, enhanced yellow fluorescent protein; FRAP, fluorescence recovery after photobleaching; GFP, green fluorescent protein; GPCR, G-protein-coupled receptor; GTP-γ-S, guanosine 5′-*O*-(3-thiotriphosphate); IBMX, 3-isobutyl-1-methylxanthine; PBS, phosphate-buffered saline; PCR, polymerase chain reaction; *p*-MPPI, 4-(2′-methoxy)phenyl-1-[2′-(*N*-2″-pyridinyl)-*p*-iodobenzamido]ethylpiperazine; *p*-MPPF, 4-(2′-methoxy)phenyl-1-[2′-(*N*-2″-pyridinyl)-*p*-fluorobenzamido]ethylpiperazine; PMSF, phenylmethanesulfonyl fluoride.

10.1021/bi0480887 CCC: $27.50
Published on Web 11/25/2004

by diffusion rates of the receptor in the membrane (*6*). This model has evolved and assumes relevance due to novel findings on G-protein-coupled signal transduction events. Recent evidence has indicated that receptors and G-proteins are less dynamic than previously appreciated. A spatiotemporally organized system rather than a freely diffusible system has been suggested to be responsible for rapid and specific propagation of extracellular stimuli to intracellular signaling molecules (*7*, *8*). Moreover, the specificity of signaling in intact cells appears to be significantly greater than that observed in reconstituted systems. In addition, the observation that G-proteins themselves are largely immobile on the plane of the plasma membrane even upon receptor activation (*9*) suggests a strong degree of clustering and therefore a controlled access to receptors on the cell surface. On the basis of these results, it has been proposed that GPCRs are not uniformly present on the plasma membrane but are concentrated in specific membrane microdomains (*7*−*11*). This heterogeneous distribution of GPCRs into domains has given rise to new challenges and complexities in receptor signaling since signaling now has to be understood in the context of the three-dimensional organization of various signaling components which include receptors and G-proteins (*11*).

Serotonin (5-hydroxytryptamine or 5-HT) is an intrinsically fluorescent neurotransmitter (*12*) and exerts its actions by binding to distinct membrane receptors that have been classified into many groups (*13*). Serotonergic signaling appears to play a key role in the generation and modulation of various cognitive, behavioral, and developmental processes in higher eukaryotes (*14*−*16*). Serotonin receptors are members of a superfamily of seven transmembrane domain receptors that couple to G-proteins (*1*). Among the 14 subtypes of serotonin receptors, the G-protein-coupled 5-HT$_{1A}$ receptor subtype is the most extensively studied for a number of reasons (*17*). One of the main reasons is the availability of a selective ligand, 8-OH-DPAT, that allows extensive biochemical, physiological, and pharmacological characterization of the receptor (*18*). In addition, this receptor was the first among serotonin receptors to be cloned and sequenced (*19*, *20*). Importantly, the 5-HT$_{1A}$ receptor levels and function have been shown to be important indices to diagnose several psychological disorders. These include alterations in the receptor levels in schizophrenia and depression (*21*, *22*) and polymorphisms in the upstream repressor region of the 5-HT$_{1A}$ receptor gene in major depression and suicide in humans (*23*). The 5-HT$_{1A}$ receptor has recently been shown to have a role in neural development (*15*) and protection of stressed neuronal cells undergoing degeneration and apoptosis (*24*). In addition, 5-HT$_{1A}$ receptor antagonists represent a major class of molecules with potential therapeutic effects in anxiety- or stress-related disorders (*25*). We have earlier shown modulation of ligand binding activity of the 5-HT$_{1A}$ receptor isolated from the bovine hippocampus with agents that perturb G-proteins (*26*, *27*), local anesthetics (*28*), and membrane cholesterol (*29*, *30*). In addition, we have solubilized and partially purified the 5-HT$_{1A}$ receptor from both the native bovine hippocampus (*17*) and heterologously expressed human 5-HT$_{1A}$ receptors from Chinese hamster ovary cells (*31*), where the receptor was found to possess very similar pharmacological characteristics as in the native system (*32*).

In this paper, we describe the characteristics of the human 5-HT$_{1A}$ receptor tagged to the red-shifted emission variant of green fluorescent protein (GFP), the enhanced yellow fluorescent protein (EYFP, previously known as GFP-10C) (*33*), stably expressed in CHO cells. The EYFP variant is advantageous since it avoids cellular autofluorescence, is relatively photostable, and has a high quantum yield (*33*). In light of the proposed significance of a spatiotemporally restricted environment in modulating receptor and G-protein interaction (see above), we have utilized the intrinsic fluorescence of the EYFP-tagged receptor to analyze its cell surface dynamics (diffusion characteristics) using the technique of fluorescence recovery after photobleaching (FRAP). On the basis of the analysis of the FRAP data, we provide evidence, for the first time, that cell surface dynamics of this receptor is altered upon receptor-dependent or -independent activation of G-proteins in an intact cellular environment. These results provide novel information on signaling events involving the 5-HT$_{1A}$ receptor.

EXPERIMENTAL PROCEDURES

Materials. 8-OH-DPAT, *p*-MPPI, penicillin, streptomycin, gentamycin sulfate, serotonin, polyethylenimine, mastoparan, and pertussis toxin were obtained from Sigma (St. Louis, MO). D-MEM/F-12 [Dulbecco's modified Eagle medium: nutrient mixture F-12 (Ham) (1:1)], lipofectamine, fetal calf serum, and geneticin (G 418) were from Invitrogen Life Technologies (Carlsbad, CA). GTP-γ-S was from Roche Applied Science (Mannheim, Germany). The BCA reagent kit for protein estimation was from Pierce (Rockford, IL). Forskolin and IBMX were obtained from Calbiochem (San Diego, CA). [^{3}H]8-OH-DPAT (specific activity = 135.0 Ci/mmol) and [^{3}H]*p*-MPPF (specific activity = 70.5 Ci/mmol) were purchased from DuPont New England Nuclear (Boston, MA). The cyclic [^{3}H]AMP (TRK 432) assay kit was purchased from Amersham Biosciences (Buckinghamshire, U.K.). GF/B glass microfiber filters were from Whatman International (Kent, U.K.). All other chemicals used were of the highest available purity. Water was purified through a Millipore (Bedford, MA) Milli-Q system and used throughout.

Construction of the 5-HT$_{1A}$R-EYFP Fusion Expression Vector. The EYFP coding sequence was fused in frame at the C-terminal end of the 5-HT$_{1A}$ receptor coding sequence. Two synthetic oligonucleotide primers were designed for PCR amplification of the 5-HT$_{1A}$ coding sequence (*19*) and cloned into the *Nhe*I/*Age*I site of the pEYFP-N1 vector (BD Biosciences Clontech, Palo Alto, CA). The sense primer, GTCGGGCTAGCCACCATGGATGTGCTCAG-CCCTGG, encoded the *Nhe*I restriction enzyme cleavage site, the Marylin−Kozak site for translation initiation, and the first 20 nucleotides of the sense strand of the 5-HT$_{1A}$ coding sequence. The antisense primer, CACCATGGTG-GCGACCGGTTGGCGGCAGAAGTTACAC, encoded the last 19 nucleotides of the antisense strand of the 5-HT$_{1A}$ receptor coding sequence followed by the *Age*I recognition sequence and 12 nucleotides of the antisense strand of the EYFP coding sequence. Both of the oligonucleotides were synthesized by Gibco BRL (Grand Island, NY). The intronless human genomic clone G-21 (*20*) in the mammalian expression vector pBC12BI was a generous gift from Dr. Probal Banerjee (College of Staten Island, City University

of New York). This insert was amplified in a PCR reaction using the above-described primers. A 1296 base pair PCR product was generated in the reaction which was cut with *Nhe*I and *Age*I and purified by agarose gel electrophoresis followed by the Promega Wizard Plus DNA purification system (Madison, WI). This pure DNA fragment was ligated to the large (4.7 kb) fragment of the pEYFP-NI vector generated upon digestion with *Nhe*I and *Age*I. *Escherichia coli* DH5α cells were transformed with this ligation mixture, and plasmids were isolated from kanamycin-resistant clones. The ~1.3 kb insert released upon digestion of this plasmid with *Nhe*I and *Age*I was sequenced at the Lerner Research Institute core facility. Clones that yielded the designed in frame fusion between the coding sequence of the 5-HT_{1A} receptor and EYFP were isolated. Plasmids were routinely purified using a Qiagen column (Qiagen, Valencia, CA) and used for transfection experiments.

Transient and Stable Transfection of CHO-K1 Cells. CHO-K1 cells were maintained in D-MEM/F-12 (1:1) supplemented with 2.4 g/L sodium bicarbonate, 10% fetal calf serum, 60 μg/mL penicillin, 50 μg/mL streptomycin, and 50 μg/mL gentamycin sulfate in a humidified atmosphere with 5% CO_2 at 37 °C. Cells grown to ~80% confluency in 35 mm dishes were transfected with 1 μg of the 5-HT_{1A}R-EYFP construct and 6 μL of lipofectamine as per the manufacturer's instructions. Two days after transfection, the cells were trypsinized and plated at a low density on 100 mm dishes with D-MEM/F12 medium containing 1 mg/mL G 418. After 1 week, the few colonies that grew were picked and transferred into six-well plates for propagation in D-MEM/F12 medium containing 0.3 mg/mL G 418. The colonies were subsequently chosen for further analysis on the basis of their fluorescence intensities. The characterization of the 5-HT_{1A}R-EYFP expressed in one such clone is described in this report.

Cell Membrane Preparation. Cell membranes were prepared as described earlier (*32*) with a few modifications. Confluent cells grown in 162 cm^2 flasks were harvested with PBS containing 0.5 mM EDTA at room temperature. Cell pellets were stored at −70 °C until further use. Pellets were thawed and homogenized in ice-cold 10 mM Tris, 5 mM EDTA, and 0.1 mM PMSF, pH 7.4, buffer with a Polytron homogenizer for 20 s at 4 °C at maximum speed. This cell lysate was centrifuged at 500*g* for 10 min at 4 °C, and the resulting postnuclear supernatant was centrifuged at 40000*g* for 30 min at 4 °C. The pellet thus obtained was suspended in 50 mM Tris, pH 7.4, buffer and used for radioligand binding studies. The total protein concentration of cell membranes was determined using the BCA assay kit.

Radioligand Binding Assays. Receptor binding assays were carried out as described earlier (*32*) with some modifications. Briefly, tubes in duplicate with 20 μg of total protein in a volume of 1 mL of buffer A (50 mM Tris, 1 mM EDTA, 10 mM $MgCl_2$, 5 mM $MnCl_2$, pH 7.4) for agonist binding or in 1 mL of buffer B (50 mM Tris, 1 mM EDTA, pH 7.4) for antagonist binding assays were used. Tubes were incubated with the radiolabeled agonist [^{3}H]8-OH-DPAT (final concentration in the assay tube 0.29 nM) or antagonist [^{3}H]*p*-MPPF (final concentration in the assay tube 0.5 nM) for 1 h at room temperature (25 °C). Nonspecific binding was determined by performing the assay either in the presence of 10 μM serotonin (for agonist binding assays) or in the presence of 10 μM *p*-MPPI (for antagonist binding assays). The binding reaction was terminated by rapid filtration under vacuum in a Brandel cell harvester (Gaithersburg, MD) through Whatman GF/B 2.5 cm diameter glass microfiber filters (1.0 μm pore size) which were presoaked in 0.15% (w/v) polyethylenimine for 1 h. The filters were then washed three times with 3 mL of cold water (4 °C) and dried, and the retained radioactivity was measured in a Packard Tri-Carb 1500 liquid scintillation counter using 5 mL of scintillation fluid.

GTP-γ-S Sensitivity Assay. For experiments in which GTP-γ-S was used, ligand binding assays were performed in the presence of varying concentrations of GTP-γ-S in buffer A containing 0.29 nM [^{3}H]8-OH-DPAT for agonist and buffer B containing 0.5 nM [^{3}H]*p*-MPPF with 2 mM $MgCl_2$ for antagonist binding studies. The concentration of GTP-γ-S leading to 50% inhibition of specific agonist binding (IC_{50}) was calculated by nonlinear regression fitting of the data to a four-parameter logistic function as described earlier (*29*):

$$B = \frac{a}{1 + (x/I)^s} + b \quad (1)$$

where B is the specific binding of the agonist normalized to control binding (in the absence of GTP-γ-S), x denotes the concentration of GTP-γ-S, a is the range ($y_{max} - y_{min}$) of the fitted curve on the ordinate (y-axis), I is the IC_{50} concentration, b is the background of the fitted curve (y_{min}), and s is the slope factor.

Saturation Radioligand Binding Assays. Saturation binding assays were carried out with increasing concentrations (0.1−7.5 nM) of the radiolabeled agonist [^{3}H]8-OH-DPAT and antagonist [^{3}H]*p*-MPPF under conditions as described above. Nonspecific binding was measured in the presence of 10 μM serotonin for agonist binding and 10 μM *p*-MPPI for antagonist binding. Binding data were analyzed as described previously (*29*). The dissociation constant (K_d) and maximum binding sites (B_{max}) were calculated by nonlinear regression analysis of binding data using the LIGAND program (Biosoft, Cambridge, U.K.) (*34*). Data obtained after regression analysis were used to plot graphs with the GRAFIT program version 3.09b (Erithacus Software, Surrey, U.K.).

Competition Binding Assays. Competition binding assays against the radiolabeled agonist [^{3}H]8-OH-DPAT (0.29 nM) and antagonist [^{3}H]*p*-MPPF (0.5 nM) were carried out in the presence of a range of concentrations (typically from 10^{-13} to 10^{-6} M) of the unlabeled competitor. Data for the competition assays were analyzed using eq 1 to obtain the IC_{50} concentrations of the unlabeled competitor ligand. The affinity of the competing ligand is expressed as its apparent inhibition constant K_i, calculated using the Cheng−Prusoff equation (*35*):

$$K_i = IC_{50}/[1 + ([L]/K_d)] \quad (2)$$

where IC_{50} is the concentration of the competing ligand leading to 50% inhibition of specific binding and [L] and K_d are the concentration and dissociation constant of the labeled ligand. K_d values are those determined from saturation binding assays for the respective radioligand.

Estimation of cAMP Levels in Cells. The ability of ligands to affect the forskolin-stimulated increase in cAMP levels

in cells was assessed. CHO-K1 cells stably expressing the 5-HT$_{1A}$R-EYFP were plated at a density of 2×10^5 cells in 35 mm dishes and grown in D-MEM/F-12 medium for 48 h. Cells were rinsed with PBS and incubated with 10 μM forskolin in the presence of 5-HT (10 μM), *p*-MPPI (10 μM), or their combination at 37 °C for 30 min in HEPES−Hanks buffer, pH 7.4. The phosphodiesterase inhibitor IBMX (50 μM) was present during this treatment. After this incubation, cells were lysed in 10 mM Tris and 5 mM EDTA, pH 7.4, buffer. Cell lysates were boiled for 3 min and spun in a microcentrifuge to remove precipitated proteins. cAMP amounts in an aliquot of the supernatant were estimated using the cyclic [^{3}H]AMP assay system (Amersham), which is based on the protein binding method described previously (*36*).

Confocal Microscopy and Live Cell Imaging. CHO-5-HT$_{1A}$R-EYFP cells were plated at a density of 5×10^4 cells on a 40 mm glass coverslip and were grown in D-MEM/F-12 medium for 72 h. Coverslips were washed twice with 3 mL of HEPES−Hanks, pH 7.4, buffer and mounted on an FCS2 closed temperature controlled Bioptechs chamber (Butler, PA). The chamber was gently perfused with 10 mL of the same buffer containing the indicated concentrations of ligands/reagents and was allowed to attain 37 °C, which took ~10 min. Cells were treated with 10 μM mastoparan in the same buffer (4 mL) for 5 min at 25 °C, mounted on the FCS2 stage, and allowed to reach 37 °C before experiments. Cells were grown in the presence of pertussis toxin (200 ng/mL) for 24 h before experiments. Images were acquired on an inverted Zeiss LSM 510 Meta confocal microscope (Jena, Germany), with a 63×, 1.2 NA water-immersion objective using the 514 nm line of an argon laser. Fluorescence emission was collected using the 535−590 nm band-pass filter. Images were recorded at a 225 μm pinhole resolution, giving an optimal *z*-slice thickness of 1.7 μm. The digital zoom was set at 2, which gave a scaling factor of 0.14 μm per image pixel. Time-lapse images were acquired under these chamber conditions and microscope settings for the desired duration of time for fluorescence distribution analysis of 5-HT$_{1A}$R-EYFP in the presence of ligands and for fluorescence photobleaching experiments.

Fluorescence Recovery after Photobleaching (*FRAP*) *Analysis.* FRAP experiments were carried out on cells that were maintained under conditions described above in the presence or absence of the indicated ligands/reagents at 37 °C in the FCS2 Bioptechs chamber. FRAP experiments were carried out ~5 min after the temperature in the chamber reached 37 °C and were complete within 30 min. The uniformly fluorescent surface of well-spread CHO-K1 cells stably expressing 5-HT$_{1A}$R-EYFP in contact with the glass coverslip was imaged for bleaching and monitoring fluorescence recovery. In a typical experiment, a square region of interest (ROI) with dimensions corresponding to 14 μm × 14 μm was scanned. Another circular region of interest, within this scanned ROI, with a radius of 1.4 μm was chosen as the bleach ROI. The time interval between successive scans was ~0.63 s. Analysis with a control ROI drawn a fair distance away from the bleach ROI indicated no significant bleach while fluorescence recovery was monitored. Data representing the mean fluorescence intensity of the bleached ROI were background subtracted using an ROI placed outside the cell boundary and were analyzed to determine the diffusion coefficient (*D*). FRAP recovery plots were analyzed on the basis of the equation for a uniform disk illumination condition (*37*):

$$F(t) = [F(\infty) - F(0)][\exp(-2\tau_d/t)(I_0(2\tau_d/t) + I_1(2\tau_d/t))] + F(0) \quad (3)$$

where $F(t)$ is the mean background corrected and normalized fluorescence intensity at time t in the bleached ROI, $F(\infty)$ is the recovered fluorescence at time $t = \infty$, $F(0)$ is the bleached fluorescence intensity set at time $t = 0$, and τ_d is the characteristic diffusion time. I_0 and I_1 are modified Bessel functions. Diffusion coefficient (D) is determined from the equation:

$$D = \omega^2/4\tau_d \quad (4)$$

where ω is the actual radius of the bleached ROI. Mobile fraction estimates of the fluorescence recovery were obtained from the equation:

$$\text{mobile fraction} = [F(\infty) - F(0)]/[F(p) - F(0)] \quad (5)$$

where $F(p)$ is the mean background corrected and normalized prebleach fluorescence intensity. Nonlinear curve fitting of the recovery data to eq 3 was carried out using Graphpad Prism software version 4.00 (San Diego, CA). Significance levels were estimated by one-way ANOVA using Microcal Origin software version 5.0 (OriginLab Corp., Northampton, MA).

RESULTS

Pharmacological Characterization of 5-HT$_{1A}$R-EYFP. CHO-K1 cells were transfected with the construct coding for the 5-HT$_{1A}$ receptor tagged to EYFP at its C-terminus. As has been shown for other GPCRs, this represents the most suitable strategy for tagging these receptors with a fluorescent reporter protein and ensures minimal perturbation of the intrinsic function of these receptors (*38*). The fluorescence intensity and ligand binding characteristics of a selected transfected clone were retained upon several passages, indicating that these were stable transfectants. Cells imaged at a mid-plane section with a confocal microscope display typical plasma membrane localization characterized by greater fluorescence intensity at the cell periphery (see Figure 5). The fluorescence intensity within these cells might represent newly synthesized proteins present in intracellular membranes as this intensity reduces upon cyclohexamide treatment (data not shown).

We have pharmacologically characterized binding of the selective 5-HT$_{1A}$ receptor agonist [^{3}H]8-OH-DPAT and antagonist [^{3}H]*p*-MPPF to cell membranes prepared from the isolated CHO clone that stably expresses 5-HT$_{1A}$R-EYFP. The saturation binding analyses of the specific agonist [^{3}H]8-OH-DPAT and antagonist [^{3}H]*p*-MPPF binding to 5-HT$_{1A}$R-EYFP receptors are shown in Figure 1 and Table 1. Importantly, the estimated K_d values of 1.07 nM for [^{3}H]8-OH-DPAT and 6.7 nM for [^{3}H]*p*-MPPF binding to 5-HT$_{1A}$R-EYFP receptors are similar to the K_d values of the untagged form of the receptor expressed in CHO cells (K_d for [^{3}H]8-OH-DPAT binding = 0.38 nM and for [^{3}H]*p*-MPPF binding = 3.51 nM) (*32*). Moreover, this is in agreement with the

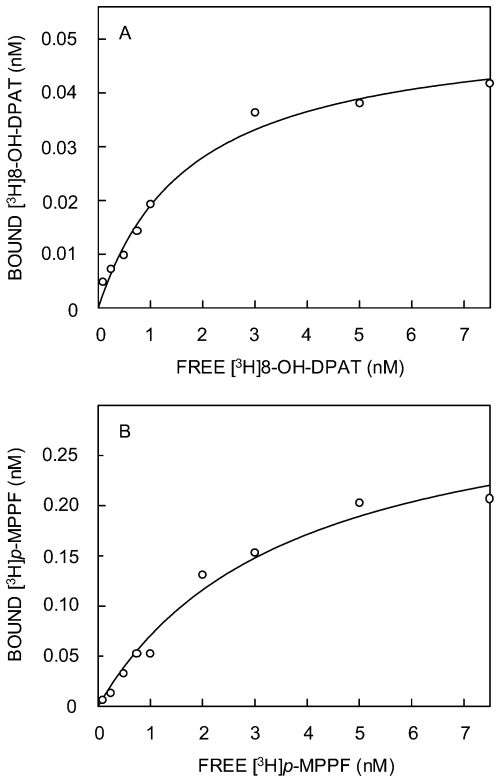

FIGURE 1: Saturation binding analysis of specific radiolabeled agonist and antagonist binding to 5-HT_{1A}R-EYFP. Cell membranes were isolated from CHO-K1 cells stably expressing 5-HT_{1A}R-EYFP. (A) A representative plot for specific [^{3}H]8-OH-DPAT binding with increasing concentrations (0.1−7.5 nM) of free [^{3}H]8-OH-DPAT is shown. (B) A representative plot for specific [^{3}H]*p*-MPPF binding with increasing concentrations (0.1−7.5 nM) of free [^{3}H]*p*-MPPF is shown. The curves are nonlinear regression fits to the experimental data. See Experimental Procedures and Table 1 for other details.

Table 1: Binding Parameters[a] of the Agonist [^{3}H]8-OH-DPAT and Antagonist [^{3}H]*p*-MPPF Binding to 5-HT_{1A}R-EYFP Expressed in CHO-K1 Cells

ligand	K_d (nM)	B_{max} (pmol/mg of protein)
[^{3}H]8-OH-DPAT	1.07 ± 0.11	2.11 ± 0.13
[^{3}H]*p*-MPPF	6.70 ± 0.77	23.67 ± 2.05

[a] Binding parameters were calculated by analyzing saturation binding isotherms with a range (0.1−7.5 nM) of both radioligands. The data shown in the table represent the means ± standard error of three independent experiments. See Experimental Procedures for other details.

K_d values for native bovine hippocampal 5-HT_{1A} receptor (*26*, *28*) and with other reports describing recombinant 5-HT_{1A} receptors (*39*).

Most of the seven transmembrane domain receptors are coupled to G-proteins (*1*), and thus guanine nucleotides are known to modulate ligand binding. The 5-HT_{1A} receptor agonists such as 5-HT and 8-OH-DPAT are known to specifically activate the G_i/G_o class of G-proteins in CHO cells (*40*). In contrast, the antagonist *p*-MPPF and its analogue *p*-MPPI do not catalyze the activation of G-proteins (*41*), although *p*-MPPI has recently been shown to be a partial inverse agonist of 5-HT_{1A} receptors (*42*). Therefore, agonist binding to such receptors displays sensitivity to agents such as GTP-γ-S that uncouple the normal cycle of guanine nucleotide exchange at the Gα subunit caused by receptor activation. We have previously shown that the

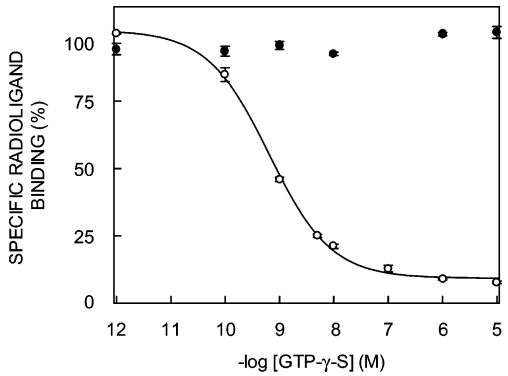

FIGURE 2: Sensitivity of radiolabeled agonist and antagonist binding to GTP-γ-S for 5-HT_{1A}R-EYFP. The data points represent the specific binding of the agonist [^{3}H]8-OH-DPAT (○) and antagonist [^{3}H]*p*-MPPF (●) to 5-HT_{1A}R-EYFP in the presence of increasing concentrations of GTP-γ-S. Values are expressed as a percentage of the specific binding obtained in the absence of GTP-γ-S. The curve associated with [^{3}H]8-OH-DPAT binding is a nonlinear regression fit to the experimental data using eq 1, and the IC_{50} value thus obtained was ~0.64 nM. The data points represent means ± standard error of duplicate points from three independent experiments. See Experimental Procedures for other details.

specific binding of the agonist [^{3}H]8-OH-DPAT to bovine hippocampal 5-HT_{1A} receptors is sensitive to guanine nucleotides and is inhibited with increasing concentrations of GTP-γ-S whereas that of the antagonist [^{3}H]*p*-MPPF is not (*26*, *27*). Our results showed that, in the presence of GTP-γ-S, 5-HT_{1A} receptors undergo an affinity transition, from a high-affinity G-protein coupled to a low-affinity G-protein uncoupled state (*26*). In agreement with these results, Figure 2 shows a characteristic reduction in binding of the agonist [^{3}H]8-OH-DPAT in the presence of a range of concentrations of GTP-γ-S with an estimated half-maximal inhibition concentration (IC_{50}) of 0.64 ± 0.04 nM (in comparison, the IC_{50} for the untagged receptor is ~3.7 nM) (*32*). The binding of the antagonist [^{3}H]*p*-MPPF remains unaffected under similar conditions. This indicates that the presence of the EYFP tag at the C-terminus of the 5-HT_{1A} receptor does not affect its ability to couple to G-proteins.

Further characterization of specific agonist and antagonist binding was carried out by performing competition binding experiments in the presence of unlabeled ligands which act as competitors. Figure 3 shows the competition displacement curves of the specific agonist [^{3}H]8-OH-DPAT by 5-HT and of the antagonist [^{3}H]*p*-MPPF by its analogue *p*-MPPI for 5-HT_{1A}R-EYFP in cell membranes. The IC_{50} values and inhibition constants (K_i) for the competing ligands are shown in Table 2. Importantly, these K_i values are in good agreement with a similar analysis carried out with the untagged form of the receptor (K_i for 5-HT against [^{3}H]8-OH-DPAT is 0.36 nM and for *p*-MPPI against [^{3}H]*p*-MPPF is 4.4 nM) (*32*). These data indicate that 5-HT, the natural agonist for the receptor, and *p*-MPPI, the iodinated analogue of the antagonist *p*-MPPF, bind to 5-HT_{1A}R-EYFP with affinities similar to that seen for the classical agonist [^{3}H]8-OH-DPAT and antagonist [^{3}H]*p*-MPPF, respectively.

Ligand-Dependent Downstream Signaling of 5-HT_{1A}R-EYFP. We examined the function of 5-HT_{1A}R-EYFP beyond its ligand binding properties and monitored its ability to catalyze downstream signal transduction processes upon stimulation with 5-HT_{1A} receptor ligands. The 5-HT_{1A}

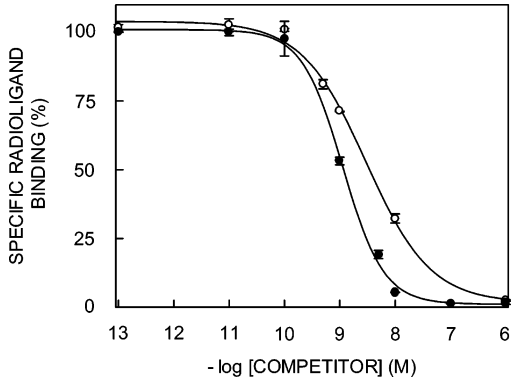

FIGURE 3: Competition binding analysis of specific agonist and antagonist binding to 5-HT$_{1A}$R-EYFP. The plots represent specific binding of [^{3}H]8-OH-DPAT (0.29 nM final concentration) in the presence of a range of concentrations of 5-HT (○) and specific binding of [^{3}H]*p*-MPPF (0.5 nM final concentration) in the presence of a range of concentrations of *p*-MPPI (●). Values are expressed as a percentage of specific binding obtained in the absence of the competing ligand. The curves are nonlinear regression fits to the experimental data using eq 1. The data points represent means ± standard error of duplicate points from three independent experiments. See Experimental Procedures and Table 2 for other details.

Table 2: Competition Binding Analysis[a] of [^{3}H]8-OH-DPAT and [^{3}H]*p*-MPPF Binding to 5-HT$_{1A}$R-EYFP Expressed in CHO-K1 Cells

competing ligand	IC_{50} (nM)	K_i (nM)
5-HT	3.01 ± 0.26	2.37 ± 0.21
p-MPPI	1.09 ± 0.09	1.02 ± 0.09

[a] Competition binding data were analyzed using eq 1 to determine IC_{50} values. The K_i values were obtained using eq 2 for which the K_d values were obtained from Table 1. Binding of [^{3}H]8-OH-DPAT (0.29 nM) was competed out with a range of concentrations of 5-HT. Binding of [^{3}H]*p*-MPPF (0.5 nM) was competed out with a range of concentrations of *p*-MPPI. The data represent the means ± standard error of three independent experiments. See Experimental Procedures for other details.

receptor agonists such as 5-HT and 8-OH-DPAT are known to specifically activate the G_i/G_o class of G-proteins in CHO cells (*40*), which subsequently reduce the cAMP levels in cells. As shown in Figure 4, the forskolin-stimulated increase in cAMP levels (shown as b) is efficiently inhibited by 5-HT (shown as c). This indicates that the normal function of these receptors to transduce signals via G-proteins which inhibit adenylate cyclase is retained upon tagging these receptors to EYFP. The addition of *p*-MPPI itself does not inhibit the forskolin-stimulated increase, and the levels of cAMP were found to be higher (shown as d) over that found with forskolin. Importantly, the effect of serotonin to reduce the forskolin-stimulated cAMP levels can be inhibited by *p*-MPPI (shown as e), confirming its antagonistic action on 5-HT$_{1A}$R-EYFP receptors.

Fluorescence Distribution of 5-HT$_{1A}$R-EYFP upon Ligand Occupation. The fluorescence distribution of 5-HT$_{1A}$R-EYFP stably expressed in CHO-K1 cells was observed at 37 °C before and after 30 min of exposure to the indicated ligand (shown in Figure 5). While the previous analyses indicate that 5-HT and *p*-MPPI display high-affinity binding to the receptor (see Table 2), analyses of several independent images taken before and after ligand addition do not indicate a significant redistribution of fluorescence of the 5-HT$_{1A}$R-EYFP in the presence of these ligands when monitored for

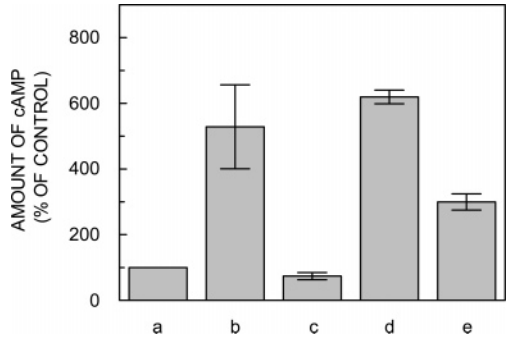

FIGURE 4: Estimation of cAMP levels in CHO-K1 cells stably expressing 5-HT$_{1A}$R-EYFP in the presence of 5-HT$_{1A}$ receptor ligands. The ability of ligands to affect the forskolin-stimulated increase in cAMP levels in cells was assessed. cAMP levels in cells were estimated as described in Experimental Procedures. Cells incubated with HEPES−Hanks buffer with 50 μM IBMX served as a control (shown in a). Cells were incubated with HEPES−Hanks buffer with 50 μM IBMX containing (b) forskolin (10 μM), (c) 5-HT (10 μM) + forskolin (10 μM), (d) *p*-MPPI (10 μM) + forskolin (10 μM), and (e) 5-HT (10 μM) + *p*-MPPI (10 μM) + forskolin (10 μM). The data are normalized to cAMP levels present in control (a) cells and represent the means ± standard error of three independent experiments.

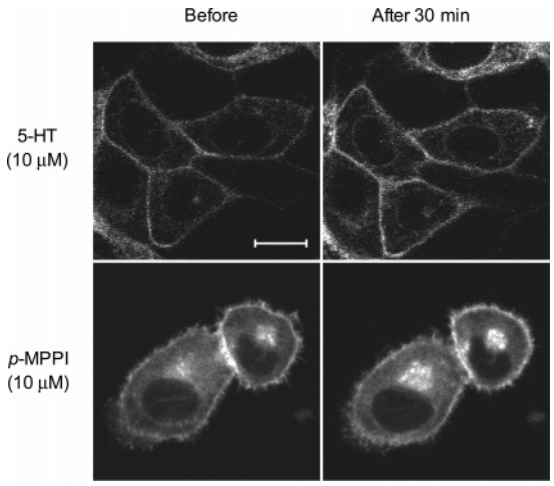

FIGURE 5: Cell surface distribution of 5-HT$_{1A}$R-EYFP in the presence of 5-HT$_{1A}$ receptor ligands. The panels show typical fluorescence distribution of 5-HT$_{1A}$R-EYFP in the same group of cells stably expressing 5-HT$_{1A}$R-EYFP before and after 30 min of exposure to the indicated ligands. Fluorescence images of cells grown on coverslips and placed in the Bioptechs FCS2 closed chamber system were acquired at 37 °C in the presence of HEPES−Hanks buffer containing the indicated concentrations of ligands. The images represent mid-plane confocal sections of the cells under conditions as described in Experimental Procedures. The scale bar represents 10 μm. See Experimental Procedures for other details.

a period of 30 min. These results set up the background for the experiments described below to assess diffusion characteristics of the receptor by FRAP as they indicate that the analysis of fluorescence recovery is not complicated by any significant alteration in the distribution of receptors in the presence of these ligands during these experiments.

Fluorescence Recovery after Photobleaching (*FRAP*) *Analysis of 5-HT$_{1A}$R-EYFP.* Fluorescence recovery after photobleaching involves generating a concentration gradient of fluorescent molecules by irreversibly photobleaching a fraction of fluorophores in the sample region. The dissipation of this gradient with time owing to diffusion of fluorophores

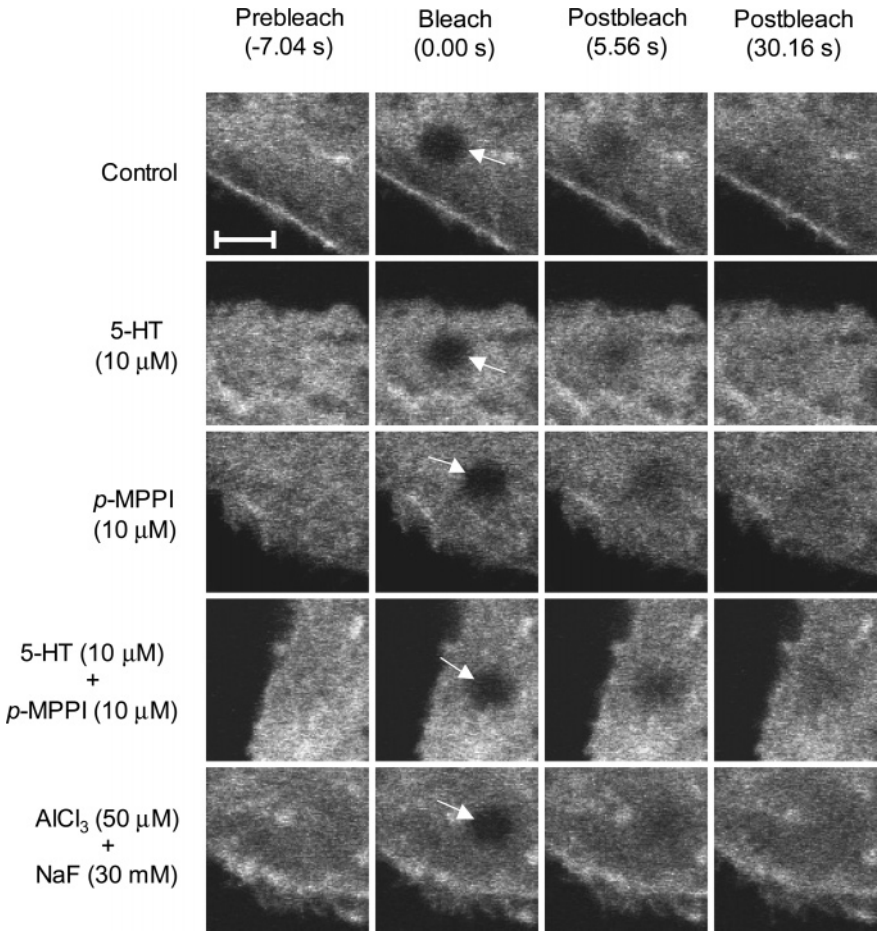

FIGURE 6: Recovery of fluorescence intensity after bleaching of 5-HT_{1A}R-EYFP in the presence of ligands or an activator of G-proteins. The panels show fluorescence intensity before and after bleaching monitored for the indicated time periods. Fluorescence images of cells grown on coverslips and placed in the Bioptechs FCS2 closed chamber system were acquired at 37 °C in the presence of HEPES−Hanks buffer containing the indicated concentrations of ligands or the G-protein activator, AlF_4^-. The images represent confocal sections of the base of the cells. Arrows indicate the region of bleach. The recovery kinetics can be qualitatively appreciated by the fluorescence recovered into the bleached spot, which is especially rapid for cells treated with AlF_4^-. The scale bar represents 5 μm. See Experimental Procedures for other details.

into the bleached region from the unbleached regions in the membrane is an indicator of the mobility of the fluorophores in the membrane. A representative panel of images demonstrating the recovery of fluorescence after photobleaching is shown in Figure 6. The homogeneity in fluorescence distribution on the surface before bleaching is an important assumption in these experiments to arrive at reliable diffusion coefficient values (*43*, *44*). Figure 6 shows that this assumption is valid in these experiments. Representative FRAP recovery plots with regression fits to the data are shown in Figure 7A. Curve fitting analysis of the recovery plots indicates a mean diffusion coefficient (D) of $(7.7 \pm 0.4) \times 10^{-10}$ cm^2 s^{-1} (mean ± SE) for 5-HT_{1A}R-EYFP receptors at 37 °C (shown as a in Figure 7B) with a mobile fraction of ~80%. This value compares well with earlier estimates of diffusion of membrane proteins equivalent in size to GPCRs in cells (*44*). It is worth mentioning here that a similar analysis of diffusion rates of pure GFP in 90% glycerol−water mixture at 25 °C gave a mean D of $\sim 0.63 \times 10^{-8}$ cm^2 s^{-1} (T. J. Pucadyil and A. Chattopadhyay, unpublished observations), which is similar to the value of 0.7×10^{-8} cm^2 s^{-1} calculated for GFP using the Stokes−Einstein equation in a medium of viscosity corresponding to 90% glycerol−water mixture (*45*), thus validating our method of analysis.

Interestingly, acute treatment of cells with 10 μM serotonin shows a significant ($P < 0.05$) increase in diffusion coefficient of 5-HT_{1A}R-EYFP to $(9.3 \pm 0.9) \times 10^{-10}$ cm^2 s^{-1} (shown as d in Figure 7B) with a mobile fraction of ~77%. The treatment of cells with 10 μM antagonist *p*-MPPI does not substantially alter the diffusion coefficient [$D = (7.2 \pm 0.5) \times 10^{-10}$ cm^2 s^{-1}; see b in Figure 7B with a mobile fraction of ~72%]. In addition, the observed increase in the diffusion coefficient of 5-HT_{1A}R-EYFP with serotonin can be reversed upon addition of 10 μM *p*-MPPI [$D = (7.8 \pm 0.9) \times 10^{-10}$ cm^2 s^{-1}; see c in Figure 7B]. The increase in diffusion of the receptor with the agonist serotonin, but not with the antagonist *p*-MPPI, prompted us to investigate these results from the point of view of G-protein activation. We explored the possibility whether activation of G-proteins independently could increase the diffusion of these receptors. The cationic peptide mastoparan has been shown to catalyze $G_{i/o}$-protein activation in a manner similar to that mediated by the G-protein-coupled receptors (*46*). The treatment of cells with mastoparan increases ($P < 0.05$) the diffusion of 5-HT_{1A}R-EYFP to levels similar to that seen with serotonin [$D = (9.2 \pm 0.5) \times 10^{-10}$ cm^2 s^{-1}; see e in Figure 7B with a mobile fraction of ~84%]. It has been proposed that AlF_4^- mimics the γ-phosphate of GTP in the guanine nucleotide binding site of the GDP-bound Gα subunit (*47*) and that it

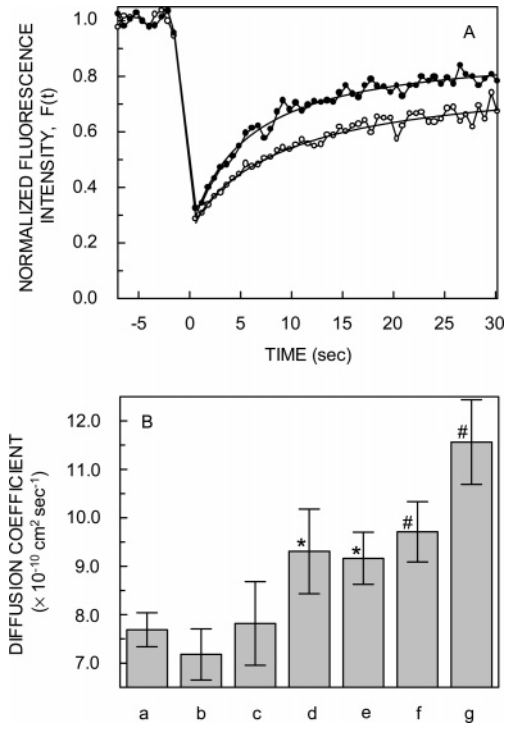

FIGURE 7: Analysis of fluorescence recovery after photobleaching (FRAP) data. (A) Typical recovery plots of 5-HT$_{1A}$R-EYFP stably expressed in CHO-K1 cells in the absence (○) or presence (●) of 50 μM $AlCl_3$ + 30 mM NaF are shown. The prebleach intensities are shown at time $t < 0$. The curves are nonlinear regression fits to the data using eq 3. (B) Diffusion coefficients of 5-HT$_{1A}$R-EYFP are shown under conditions of (a) no addition (control), (b) *p*-MPPI (10 μM), (c) 5-HT (10 μM) + *p*-MPPI (10 μM), (d) 5-HT (10 μM), (e) mastoparan (10 μM), (f) cells treated with pertussis toxin (200 ng/mL), and (g) 50 μM $AlCl_3$ + 30 mM NaF. The data represent the means ± standard error of at least 11 independent experiments for each condition. The means are significantly different from control values at $P < 0.05$ (∗) and $P < 0.005$ (#). See Experimental Procedures for other details.

can mimic the effects of GTP and GTP-γ-S on G-proteins. Moreover, cell membranes are permeable to AlF_4^-, unlike GTP or GTP-γ-S, and thus are widely used to activate G-proteins in intact cells (*48*). Treatment of cells expressing the 5-HT$_{1A}$R-EYFP with AlF_4^- (50 μM $AlCl_3$ + 30 mM NaF) significantly ($P < 0.005$) increases the diffusion coefficient of 5-HT$_{1A}$R-EYFP by ~1.5-fold [$D = (11.6 \pm 0.9) \times 10^{-10}$ cm^2 s^{-1}; see g in Figure 7B with a mobile fraction of ~85%]. These results therefore suggest that receptor-independent activation of G-proteins significantly increases the diffusion rates of 5-HT$_{1A}$R-EYFP and support the possibility that the increase seen with serotonin could represent the natural agonist-induced activation of G-proteins. This activation could lead to dissociation of the G-protein from the receptor, increasing the diffusion of the latter. If this were true, then prevention of receptor and G-protein interaction per se should also lead to an increase in receptor diffusion. To achieve this, cells were treated with pertussis toxin, which ADP-ribosylates and inactivates the α subunit of the G_i and G_o class of proteins (*49*). FRAP experiments carried out on cells treated with pertussis toxin reveal an increase ($P < 0.005$) in diffusion of 5-HT$_{1A}$R-EYFP [$D = (9.7 \pm 0.6) \times 10^{-10}$ cm^2 s^{-1}; see f in Figure 7B with a mobile fraction of ~83%], thus supporting our interpretation on the increase in receptor diffusion in the presence of the agonist 5-HT. To the best of our knowledge, this is the first demonstration that the cell surface dynamics (as monitored by FRAP) of a GPCR can be modulated in a G-protein-dependent manner.

DISCUSSION

Green fluorescent protein from the jellyfish *Aequoria victoria* and its variants have become popular reporter molecules for monitoring protein expression, localization, and mobility of various membrane and cytoplasmic proteins (*50*). More specifically, tagging of GPCRs with GFP has allowed direct visualization of signaling and real-time trafficking in living cells (*51*). The use of fluorescent reporter proteins has its advantages over fluorescently labeled ligands to visualize receptors for the following reasons: (i) the stoichiometry of the receptor and fluorescent protein is well defined as the latter is covalently attached to the receptor at the DNA level, (ii) complications encountered while using fluorescent ligands such as ligand dissociation are avoided, (iii) this approach allows analysis of the unliganded states of the receptor (not possible with fluorescently labeled ligands), (iv) the possibility of perturbation induced by bulky fluorescent groups to small endogenous ligands such as biogenic amines limits their use, and (v) cellular biosynthesis ensures the presence of receptors attached to fluorescent proteins in cells and eliminates the necessity of labeling receptors with fluorescent ligands before each experiment.

We report here that the pharmacological characteristics of the 5-HT$_{1A}$ receptor are retained when attached to EYFP at its carboxy terminus. Thus the binding of the specific agonist 8-OH-DPAT and antagonist *p*-MPPF to 5-HT$_{1A}$R-EYFP and the sensitivity of ligand binding to GTP-γ-S were found to be similar to that of the untagged form of the receptor. In addition, the EYFP-tagged receptor can efficiently catalyze downstream signal transduction by reducing the cAMP levels in cells. These results demonstrate that 5-HT$_{1A}$R-EYFP receptors can be reliably used to mimic native 5-HT$_{1A}$ receptors to explore cell surface organization, distribution, and dynamics using fluorescence approaches. Furthermore, utilizing EYFP fluorescence, we have monitored the dynamics of 5-HT$_{1A}$R-EYFP on the cell surface under conditions of receptor-dependent and -independent activation of G-proteins.

The analysis of cell surface dynamics of membrane proteins such as GPCRs is crucial for a comprehensive understanding of their organization and signaling functions (*7*). Since G-proteins are by themselves membrane-anchored proteins, it is evident that cell surface dynamics of both the receptor and G-protein are important determinants of G-protein-coupled signal transduction events. To address these issues, we have carried out FRAP experiments on cells stably expressing 5-HT$_{1A}$R-EYFP. Interestingly, addition of receptor-specific ligands does not appear to elicit any significant fluorescence redistribution of the 5-HT$_{1A}$R-EYFP (Figure 5). These results are somewhat surprising since previous reports for other GPCRs tagged to fluorescent reporter proteins have shown ligand-mediated receptor internalization (*38*, *51*). Although CHO cells have been a popular system for pharmacological characterization of recombinant 5-HT$_{1A}$ receptors (*32*, *40*), internalization of 5-HT$_{1A}$ receptors in these cells has not been demonstrated. In addition, there appears

to be a lack of consensus on the ability of ligands such as 8-OH-DPAT and 5-HT to induce internalization of 5-HT_{1A} receptors expressed in other cell types. Thus, while serotonin has been shown to mediate a modest degree (~30%) of internalization of the hemagglutinin-epitope-tagged 5-HT_{1A} receptors in HEK-293 cells assessed using immunocytochemistry (*52*), studies carried out with 8-OH-DPAT using polyclonal antibodies against the receptor indicate that such a phenomenon occurs only for receptors in the neurons of the dorsal raphe nucleus but not in the hippocampus (*53*).

The observed increase in the diffusion of 5-HT_{1A}R-EYFP upon stimulation with the natural agonist serotonin and not with the antagonist *p*-MPPI suggests that activation of G-proteins makes the receptor more mobile on the cell surface. Our results on the increase in diffusion of the receptor in the presence of mastoparan and AlF_4^-, which activates G-proteins in a receptor-independent manner, provide further evidence to support this interpretation. Moreover, the treatment of cells with pertussis toxin that reduces receptor and G-protein interaction also causes an increase in receptor diffusion. Interestingly, treatment of cells with mastoparan or pertussis toxin does not appear to increase receptor diffusion to the same extent as observed with AlF_4^-. A possible reason for this difference could be that the efficacy of action (determined by the intracellular concentration and accessibility to G-proteins in a native cellular environment) of serotonin, pertussis toxin, mastoparan, and AlF_4^- may not be the same. Nevertheless, the observation of an increase in receptor diffusion upon treatment of cells with these agents reinforces our interpretation that interaction of G-proteins with the receptor could considerably affect receptor diffusion on the cell surface.

The G-protein heterotrimer is a large protein complex with an average molecular mass of ~88 kDa (*54*), which would be ~1.2 times the mass of 5-HT_{1A}R-EYFP. It is therefore possible that their association with the receptor would reduce its diffusion coefficient. Models on GPCR activation indicate that the activation process stimulates the exchange of a GTP for the existing GDP molecule at the Gα subunit of G-proteins (*54*). When this occurs, the receptor-bound G-protein heterotrimer complex dissociates until another inactive G-protein binds to the receptor. As long as the agonist is bound to the receptor, this cycle continues, eventually leading to an amplification of this cycle. A basal level of receptor activation would constitute the cyclic dissociation and association of G-proteins to the receptor in the absence of agonists. Persistent activation of the receptor with agonists, as is the case in our experiments, would on average tend to reduce the fraction of receptors interacting with G-proteins as has been recently shown (*55*). The presence of AlF_4^- would lock the Gα subunits in an active state, similar to a GTP-γ-S bound Gα subunit, preventing them from associating with the receptor (*47*, *48*) and thereby increasing the fraction of receptors uncoupled to G-proteins. The treatment of cells with pertussis toxin would inactivate the existing pool of G-proteins and increase the fraction of receptors uncoupled to G-proteins (*56*). A recent fluorescence correlation spectroscopy study carried out on rhodamine-labeled galanin bound to galanin receptors supports this possibility (*57*). Analysis of the diffusion of galanin receptor detected the presence of at least two populations of the receptor. Treatment of cells with pertussis toxin to inactivate endogenous G-proteins led to a complete loss of the slowly diffusing population which was due to receptors coupled to G-proteins (*57*).

The increase in diffusion of the receptor upon activation of G-proteins could imply that the receptors are precoupled to G-proteins under control conditions. There is physical evidence that 5-HT_{1A} receptors are precoupled to G-proteins in the absence of the agonist (*56*). It is apparent from these studies that the G-protein-coupled and uncoupled forms of the receptor are in equilibrium with each other. Agents that activate G-proteins (either receptor-dependent or -independent) therefore could shift this equilibrium toward the latter. Since fluorescence recovery after photobleaching (FRAP) experiments are carried out on a rather long time scale (typically in seconds) and the fact that FRAP monitors the average diffusion behavior of large number of receptor molecules, if a significant population of receptors were to be uncoupled from G-proteins, then the average diffusion coefficient would display an increase, as is evident from our results.

The diffusion behavior of several integral membrane proteins indicates that the cytoskeleton underlying the cell surface can act as a barrier to free diffusion of these proteins. This is thought to occur due to the steric hindrance imposed by the cytoskeleton on the cytoplasmic domains of these proteins. Treatment of cells with agents that disrupt the cytoskeleton (*58*), truncation of the cytoplasmic domains of transmembrane proteins (*59*), or a lack of interaction of membrane proteins with cytoplasmic effector molecules (*60*) tends to increase their mobility on the cell surface. Likewise, the presence of the bulky heterotrimeric G-protein complex associated with the receptor (since G-proteins, when bound to membrane receptors, could be considered as equivalent to cytoplasmic domains of membrane proteins) could reduce receptor diffusion, which would be partially relieved when the G-protein dissociates from the receptor. Another possibility could be that the increase in receptor diffusion could reflect changes in the oligomeric state of the receptor, as has been shown for the δ-opioid receptor (*61*), and the cholecystokinin receptor (*62*) or their partitioning into or out of domains proposed to exist on the cell surface (*7*, *8*, *10*, *11*).

We conclude that 5-HT_{1A}R-EYFP receptors can be reliably used to explore distribution and dynamics of the 5-HT_{1A} receptor. An important aspect of our results is that the cell surface dynamics of the receptor is modulated in a G-protein-dependent manner. The implication of such alteration in receptor dynamics on receptor function and signal transduction deserves comment. We have recently reported the effects of cholesterol depletion, a process that independently alters membrane dynamics, on receptor function and lateral diffusion characteristics (*63*, *64*). In light of growing evidence on the compartmentalized localization of G-proteins in cholesterol-rich membrane domains (*7*, *8*, *10*, *11*, *65*), our results on the G-protein-dependent cell surface dynamics of the 5-HT_{1A} receptor provide novel insight and present a sensitive and powerful approach to assess receptor/G-protein interaction in intact, unperturbed cell membranes. This approach could prove to be useful in analyzing the molecular mechanism of signal transduction of 5-HT_{1A} receptors in particular and G-protein-coupled receptors in general.

ACKNOWLEDGMENT

We gratefully acknowledge Dr. Probal Banerjee (College of Staten Island, City University of New York) for the kind gift of p-BC12B1, for CHO cells expressing the untagged form of the 5-HT$_{1A}$ receptor, and for sharing useful information. We sincerely thank Dr. G. Krishnamoorthy (Tata Institute for Fundamental Research, Mumbai, India) for the kind gift of purified GFP and Dr. Preeti G. Joshi (National Institute of Mental Health and Neurosciences, Bangalore, India) for the kind gift of pertussis toxin. We thank members of our laboratory for critically reading the manuscript.

REFERENCES

1. Pierce, K. L., Premont, R. T., and Lefkowitz, R. J. (2002) Seven-transmembrane receptors, *Nat. Rev. Mol. Cell Biol. 3*, 639−650.
2. Gether, U. (2000) Uncovering molecular mechanisms involved in activation of G protein-coupled receptors, *Endocr. Rev. 21*, 90−113.
3. Hamm, H. E. (2001) How activated receptors couple to G proteins, *Proc. Natl. Acad. Sci. U.S.A. 98*, 4819−4821.
4. Peters, R. (1988) Lateral mobility of proteins and lipids in the red cell membrane and the activation of adenylate cyclase by beta-adrenergic receptors, *FEBS Lett. 234*, 1−7.
5. Jans, D. A., et al. (1989) The adenylate cyclase-coupled vasopressin V2-receptor is highly laterally mobile in membranes of LLC-PK1 renal epithelial cells at physiological temperature, *EMBO J. 8*, 2481−2488.
6. Calvert, P. D., et al. (2001) Membrane protein diffusion sets the speed of rod phototransduction, *Nature 411*, 90−94.
7. Neubig, R. R. (1994) Membrane organization in G-protein mechanisms, *FASEB J. 8*, 939−946.
8. Hur, E.-M., and Kim, K.-T. (2002) G protein-coupled receptor signalling and cross-talk: achieving rapidity and specificity, *Cell. Signalling 14*, 397−405.
9. Kwon, G., Axelrod, D., and Neubig, R. R. (1994) Lateral mobility of tetramethylrhodamine (TMR) labelled G protein alpha and beta gamma subunits in NG 108−15 cells, *Cell. Signalling 6*, 663−679.
10. Ostrom, R. S., Post, S. R., and Insel, P. A. (2000) Stoichiometry and compartmentation in G protein-coupled receptor signaling: implications for therapeutic interventions involving G$_s$, *J. Pharmacol. Exp. Ther. 294*, 407−412.
11. Ostrom, R. S. (2002) New determinants of receptor-effector coupling: trafficking and compartmentation in membrane microdomains, *Mol. Pharmacol. 61*, 473−476.
12. Chattopadhyay, A., Rukmini, R., and Mukherjee, S. (1996) Photophysics of a neurotransmitter: ionization and spectroscopic properties of serotonin, *Biophys. J. 71*, 1952−1960.
13. Hoyer, D., Hannon, J. P., and Martin, G. R. (2002) Molecular, pharmacological and functional diversity of 5-HT receptors, *Pharmacol. Biochem. Behav. 71*, 533−554.
14. Julius, D. (1998) Serotonin receptor knockouts: a moody subject, *Proc. Natl. Acad. Sci. U.S.A. 95*, 15153−15154.
15. Gross, C., et al. (2002) Serotonin$_{1A}$ receptor acts during development to establish normal anxiety-like behaviour in the adult, *Nature 416*, 396−400.
16. Gaspar, P., Cases, O., and Maroteaux, L. (2003) The developmental role of serotonin: news from mouse molecular genetics, *Nat. Rev. Neurosci. 4*, 1002−1012.
17. Pucadyil, T. J., Kalipatnapu, S., and Chattopadhyay, A. (2004) The serotonin$_{1A}$ receptor: A representative member of the serotonin receptor family, *Cell. Mol. Neurobiol.* (in press).
18. Gozlan, H., et al. (1983) Identification of presynaptic serotonin autoreceptors using a new ligand: ^{3}H-PAT, *Nature 305*, 140−142.
19. Kobilka, B. K., et al. (1987) An intronless gene encoding a potential member of the family of receptors coupled to guanine nucleotide regulatory proteins, *Nature 329*, 75−79.
20. Fargin, A., et al. (1988) The genomic clone G-21 which resembles a beta-adrenergic receptor sequence encodes the 5-HT$_{1A}$ receptor, *Nature 335*, 358−360.
21. Sumiyoshi, T., et al. (1996) Serotonin$_{1A}$ receptors are increased in postmortem prefrontal cortex in schizophrenia, *Brain Res. 708*, 209−214.
22. Fajardo, O., et al. (2003) Serotonin, serotonin 5-HT$_{1A}$ receptors and dopamine in blood peripheral lymphocytes of major depression patients, *Int. Immunopharmacol. 3*, 1345−1352.
23. Lemonde, S., et al. (2003) Impaired repression at a 5-hydroxytryptamine 1A receptor gene polymorphism associated with major depression and suicide, *J. Neurosci. 23*, 8788−8799.
24. Adayev, T., et al. (2003) The G protein-coupled 5-HT$_{1A}$ receptor causes suppression of caspase-3 through MAPK and protein kinase Cα, *Biochim. Biophys. Acta 1640*, 85−96.
25. Griebel, G. (1999) 5-HT$_{1A}$ receptor blockers as potential drug candidates for the treatment of anxiety disorders, *Drug News Perspect. 12*, 484−490.
26. Harikumar, K. G., and Chattopadhyay, A. (1999) Differential discrimination of G-protein coupling of serotonin$_{1A}$ receptors from bovine hippocampus by an agonist and an antagonist, *FEBS Lett. 457*, 389−392.
27. Javadekar-Subhedar, V., and Chattopadhyay, A. (2004) Temperature-dependent interaction of the bovine hippocampal serotonin$_{1A}$ receptor with G-proteins, *Mol. Membr. Biol. 21*, 119−123.
28. Kalipatnapu, S., and Chattopadhyay, A. (2004) Interaction of serotonin$_{1A}$ receptors from bovine hippocampus with tertiary amine local anesthetics, *Cell. Mol. Neurobiol. 24*, 403−422.
29. Pucadyil, T. J., and Chattopadhyay, A. (2004) Cholesterol modulates ligand binding and G-protein coupling to serotonin$_{1A}$ receptors from bovine hippocampus, *Biochim. Biophys. Acta 1663*, 188−200.
30. Pucadyil, T. J., Shrivastava, S., and Chattopadhyay, A. (2004) The sterol-binding antibiotic nystatin differentially modulates ligand binding of the bovine hippocampal serotonin$_{1A}$ receptor, *Biochem. Biophys. Res. Commun. 320*, 557−562.
31. Chattopadhyay, A., Jafurulla, Md., and Kalipatnapu, S. (2004) Solubilization of serotonin$_{1A}$ receptors heterologously expressed in Chinese hamster ovary cells, *Cell. Mol. Neurobiol. 24*, 293−300.
32. Kalipatnapu, S., et al. (2004) Ligand binding characteristics of the human serotonin$_{1A}$ receptor heterologously expressed in CHO cells, *Biosci. Rep.* (in press).
33. Ormö, M., et al. (1996) Crystal structure of the Aequorea victoria green fluorescent protein, *Science 273*, 1392−1395.
34. Munson, P. J., and Rodbard, D. (1980) Ligand: a versatile computerized approach for characterization of ligand-binding systems, *Anal. Biochem. 107*, 220−239.
35. Cheng, Y.-C., and Prusoff, W. H. (1973) Relationship between the inhibition constant (K_i) and the concentration of inhibitor which causes 50% inhibition (IC_{50}) of an enzymatic reaction, *Biochem. Pharmacol. 22*, 3099−3108.
36. Norstedt, C., and Fredholm, B. B. (1990) A modification of a protein-binding method for rapid quantification of cAMP in cell-culture supernatants and body fluid, *Anal. Biochem. 189*, 231−234.
37. Soumpasis, D. M. (1983) Theoretical analysis of fluorescence photobleaching recovery experiments, *Biophys. J. 41*, 95−97.
38. Tarasova, N. I., et al. (1997) Visualization of G protein-coupled receptor trafficking with the aid of the green fluorescent protein. Endocytosis and recycling of cholecystokinin receptor type A, *J. Biol. Chem. 272*, 14817−14824.
39. Kellet, E., Carr, I. C., and Milligan, G. (1999) Regulation of G protein activation and effector modulation by fusion proteins between the human 5-hydroxytryptamine$_{1A}$ receptor and the α subunit of G$_{i1}\alpha$: differences in receptor-constitutive activity imparted by single amino acid substitutions in G$_{i1}\alpha$, *Mol. Pharmacol. 56*, 684−692.
40. Raymond, J. R., Olsen, C. L., and Gettys, T. W. (1993) Cell-specific physical and functional coupling of human 5-HT$_{1A}$ receptors to inhibitory G protein α-subunits and lack of coupling to Gsα, *Biochemistry 32*, 11064−11073.
41. Kung, M.-P., et al. (1995) 4-(2′-Methoxy-phenyl)-1-[2′-(*N*-2″-pyridinyl)-*p*-iodobenzamido]-ethyl-piperazine ([^{125}I]*p*-MPPI) as a new selective radioligand of serotonin$_{1A}$ sites in rat brain: in vitro binding and autoradiographic studies, *J. Pharmacol. Exp. Ther. 272*, 429−437.
42. Barr, A. J., and Manning, D. R. (1997) Agonist-independent activation of Gz by the 5-hydroxytryptamine$_{1A}$ receptor co-expressed in *Spodoptera frugiperda* cells. Distinguishing inverse agonists from neutral antagonists, *J. Biol. Chem. 272*, 32979−32987.
43. Petersen, N. O., Felder, S., and Elson, E. L. (1986) in *Handbook of Experimental Immunology* (Weir, D. M., Herzenberg, L. A.,

Blackwell, C. C., and Herzenberg, L. A., Eds.) p 24.1−24.23, Blackwell Scientific Publications, Edinburgh.
44. Edidin, M. (1994) in *Mobility and Proximity in Biological Membranes* (Damjanovich, S., Edidin, M., Szollosi, J., and Tron, L., Eds.) pp 109−135, CRC Press, Boca Raton, FL.
45. Kubitscheck, U., et al. (2000) Imaging and tracking of single GFP molecules in solution, *Biophys. J. 78*, 2170−2179.
46. Higashijima, T., Burnier, J., and Ross, E. M. (1990) Regulation of Gi and Go by mastoparan, related amphiphilic peptides, and hydrophobic amines. Mechanism and structural determinants of activity, *J. Biol. Chem. 265*, 14176−14186.
47. Higashijima, T., et al. (1991) ^{19}F and ^{31}P NMR spectroscopy of G protein alpha subunits. Mechanism of activation by Al^{3+} and F^-, *J. Biol. Chem. 266*, 3396−3401.
48. Inoue, Y., Fishman, P. H., and Rebois, R. V. (1990) Differential activation of the stimulatory and inhibitory guanine nucleotide-binding proteins by fluoroaluminate in cells and in membranes, *J. Biol. Chem. 265*, 10645−10651.
49. Sternweiss, P. C., and Robishaw, J. D. (1984) Isolation of two proteins with high affinity for guanine nucleotides from membranes of bovine brain, *J. Biol. Chem. 259*, 13806−13813.
50. Tsien, R. Y. (1998) The green fluorescent protein, *Annu. Rev. Biochem. 67*, 509−544.
51. Kallal, L., and Benovic, J. L. (2000) Using green fluorescent proteins to study G-protein-coupled receptor localization and trafficking, *Trends Pharmacol. Sci. 21*, 175−180.
52. Della Rocca, G. J., et al. (1999) Serotonin $5\text{-}HT_{1A}$ receptor-mediated Erk activation requires calcium/calmodulin-dependent receptor endocytosis, *J. Biol. Chem. 274*, 4749−4753.
53. Riad, M., et al. (2001) Agonist-induced internalization of serotonin-1A receptors in the dorsal raphe nucleus (autoreceptors) but not hippocampus (heteroreceptors), *J. Neurosci. 21*, 8378−8386.
54. Casey, P. J., and Gilman, A. G. (1988) G protein involvement in receptor-effector coupling, *J. Biol. Chem. 263*, 2577−2580.
55. Janetopoulos, C., Jin, T., and Devreotes, P. (2001) Receptor-mediated activation of heterotrimeric G-proteins in living cells, *Science 291*, 2408−2411.
56. Emerit, M. B., et al. (1990) Physical evidence of the coupling of solubilized $5\text{-}HT_{1A}$ binding sites with G regulatory proteins, *Biochem. Pharmacol. 39*, 7−18.
57. Pramanik, A., et al. (2001) Fluorescence correlation spectroscopy detects galanin receptor diversity on insulinoma cells, *Biochemistry 40*, 10839−10845.
58. Fujiwara, T., et al. (2002) Phospholipids undergo hop diffusion in compartmentalized cell membrane, *J. Cell Biol. 157*, 1071−1081.
59. Edidin, M., Zúñiga, M. C., and Sheetz, M. P. (1994) Truncation mutants define and locate cytoplasmic barriers to lateral mobility of membrane glycoproteins, *Proc. Natl. Acad. Sci. U.S.A. 91*, 3378−3382.
60. Zhang, F., et al. (1995) Lateral mobility of FcγRIIa is reduced by protein kinase C activation, *FEBS Lett. 376*, 77−80.
61. Cvejic, S., and Devi, L. A. (1997) Dimerization of the delta opioid receptor: implication for a role in receptor internalization, *J. Biol. Chem. 272*, 26959−26964.
62. Cheng, Z.-J., and Miller, L. J. (2001) Agonist-dependent dissociation of oligomeric complexes of G protein-coupled cholecystokinin receptors demonstrated in living cells using bioluminescence resonance energy transfer, *J. Biol. Chem. 276*, 48040−48047.
63. Kalipatnapu, S., Pucadyil, T. J., and Chattopadhyay, A. (2003) Cell surface organization and dynamics of $serotonin_{1A}$ receptors in the membrane environment, *Mol. Biol. Cell 14*, 78a.
64. Kalipatnapu, S., Pucadyil, T. J., and Chattopadhyay, A. (2004) Cell surface organization and dynamics of the $serotonin_{1A}$ receptor, *J. Gen. Physiol. 124*, 32a−33a.
65. Huang, C., et al. (1997) Organization of G proteins and adenylyl cyclase at the plasma membrane, *Mol. Biol. Cell 8*, 2365−2378.

BI0480887